AFRL-RZ-WP-TP-2010-2049

INKJET PRINTING OF ANODE SUPPORTED SOFC: COMPARISON OF SLURRY PASTED CATHODE AND PRINTED CATHODE (POSTPRINT)

Thomas L. Reitz and Ryan M. Miller

Thermal & Electrochemical Branch
Energy/Power/Thermal Division

A. M. Sukeshini and Ryan Cummins

Wright State University

FEBRUARY 2010

AIR FORCE RESEARCH LABORATORY
PROPULSION DIRECTORATE
WRIGHT-PATTERSON AIR FORCE BASE, OH 45433-7251
AIR FORCE MATERIEL COMMAND
UNITED STATES AIR FORCE

REPORT DOCUMENTATION PAGE

Form Approved
OMB No. 0704-0188

1. REPORT DATE *(DD-MM-YY)*	2. REPORT TYPE	3. DATES COVERED *(From - To)*
February 2010	Journal Article Postprint	01 January 2009 – 30 May 2009

4. TITLE AND SUBTITLE
INKJET PRINTING OF ANODE SUPPORTED SOFC: COMPARISON OF SLURRY PASTED CATHODE AND PRINTED CATHODE (POSTPRINT)

5a. CONTRACT NUMBER
In-house

5b. GRANT NUMBER

5c. PROGRAM ELEMENT NUMBER
62203F

6. AUTHOR(S)
Thomas L. Reitz and Ryan M. Miller (AFRL/RZPS)
A. M. Sukeshini and Ryan Cummins (Wright State University)

5d. PROJECT NUMBER
3145

5e. TASK NUMBER
01

5f. WORK UNIT NUMBER
314501CK

7. PERFORMING ORGANIZATION NAME(S) AND ADDRESS(ES)
Thermal & Electrochemical Branch (AFRL/RZPS)
Energy/Power/Thermal Division
Air Force Research Laboratory, Propulsion Directorate
Wright-Patterson Air Force Base, OH 45433-7251
Air Force Materiel Command, United States Air Force

Wright State University
Department of Mechanical and Materials Engineering
Dayton, OH 45430

8. PERFORMING ORGANIZATION REPORT NUMBER
AFRL-RZ-WP-TP-2010-2049

9. SPONSORING/MONITORING AGENCY NAME(S) AND ADDRESS(ES)
Air Force Research Laboratory
Propulsion Directorate
Wright-Patterson Air Force Base, OH 45433-7251
Air Force Materiel Command
United States Air Force

10. SPONSORING/MONITORING AGENCY ACRONYM(S)
AFRL/RZPS

11. SPONSORING/MONITORING AGENCY REPORT NUMBER(S)
AFRL-RZ-WP-TP-2010-2049

12. DISTRIBUTION/AVAILABILITY STATEMENT
Approved for public release; distribution unlimited.

13. SUPPLEMENTARY NOTES
Journal article published in *Electrochemical and Solid-State Letters*, Vol. 12, No. 12, 2009. PA Case Number: 88ABW-2009-2786; Clearance Date: 23 June 2009.

14. ABSTRACT
Solid oxide fuel cells (SOFCs) were fabricated by depositing NiO/yttria-stabilized zirconia (YSZ) anode interlayer, YSZ electrolyte layer, and strontium-doped lanthanum manganate (LSM)-YSZ and LSM cathode layers on a NiO–YSZ support using an inkjet printing method with potential for high reproducibility and design flexibility. The cells exhibited a stable open-circuit voltage of 1.1 V and a maximum power density of 430–460 mW/cm^2 at 850°C for hydrogen. For comparison, cells similar in all respects except for utilizing conventional hand-pasted slurry for the cathode layers, were tested and shown to have similar electrochemical performance. Altering the rheological property of the ink and/or the printing process parameter altered the microstructure of printed layers.

15. SUBJECT TERMS
solid oxide fuel cell, ink jet printing

16. SECURITY CLASSIFICATION OF:			17. LIMITATION OF ABSTRACT:	18. NUMBER OF PAGES	19a. NAME OF RESPONSIBLE PERSON (Monitor)
a. REPORT	b. ABSTRACT	c. THIS PAGE			Stanley Rodrigues
Unclassified	Unclassified	Unclassified	SAR	10	19b. TELEPHONE NUMBER *(Include Area Code)* N/A

Standard Form 298 (Rev. 8-98)
Prescribed by ANSI Std. Z39-18

Electrochemical and Solid-State Letters, **12** (12) B176-B179 (2009)
1099-0062/2009/12(12)/B176/4/$25.00 © The Electrochemical Society

Inkjet Printing of Anode Supported SOFC: Comparison of Slurry Pasted Cathode and Printed Cathode

A. M. Sukeshini,[a,z] R. Cummins,[a] T. L. Reitz,[b] and R. M. Miller[b]

[a]*Department of Mechanical and Materials Engineering, Wright State University, Dayton, Ohio 45430, USA*
[b]*Propulsion Directorate, The Air Force Research Laboratory, Wright-Patterson AFB, Ohio 45433, USA*

Solid oxide fuel cells (SOFCs) were fabricated by depositing NiO/yttria-stabilized zirconia (YSZ) anode interlayer, YSZ electrolyte layer, and strontium-doped lanthanum manganate (LSM)-YSZ and LSM cathode layers on a NiO–YSZ support using an inkjet printing method with potential for high reproducibility and design flexibility. The cells exhibited a stable open-circuit voltage of 1.1 V and a maximum power density of 430–460 mW/cm^2 at 850°C for hydrogen. For comparison, cells similar in all respects except for utilizing conventional hand-pasted slurry for the cathode layers, were tested and shown to have similar electrochemical performance. Altering the rheological property of the ink and/or the printing process parameter altered the microstructure of printed layers.
 [DOI: 10.1149/1.3243468]

Manuscript submitted July 7, 2009; revised manuscript received September 11, 2009. Published October 9, 2009.

The increasing demand for clean and efficient power generation has led to extensive research and development activities in the area of solid oxide fuel cells (SOFCs).[1-3] Conventional SOFCs designed for operation at 800°C are comprised of a yttria-stabilized zirconia (YSZ) electrolyte film (8–15 μm thick), and electrochemically active anode and cathode interlayers (<50 μm thick), and a cathode current collection layer deposited on a porous anode support. Multilayered cell configurations enable a combination of properties that are both mechanically and electrochemically superior[4-7] and enable operation at intermediate and lower temperatures. Recently, cells with more complex geometries, such as the honeycomb-type and the segmented-in-series SOFCs, have been explored.[8-10] These varied multilayered cells require precise positioning of overlapping layers. Cost effective processing methodologies are needed that can offer improved spatial control and reproducibility when compared to traditional approaches such as vacuum deposition, tape casting, and screen printing.[11,12]

Inkjet printing technology is a digital, high resolution, noncontact, direct-write material deposition method. No masks or screens are needed as it is data-driven. The printing information is created directly from computer-aided design or similar formats and is stored digitally. The surge of handheld devices, human implantable devices, and microelectromechanical systems devices has served as an impetus for a more widespread adoption of this technology.[13] Recently, it has been exploited for applications in polymer electrolyte fuel cell[14] and SOFCs.[15-17] In our preliminary study we demonstrated the fabrication of single SOFCs, where parts of the cell were inkjet-printed.[15] In a following study,[16] all nonsupported layers were inkjet-printed. The performance, however, of cells with a printed cathode interlayer and cathode current collection layer did not match the performance of cells with a hand-pasted cathode interlayer and cathode current collection layers. The poor performance was attributed to the suboptimized cathode layers. One simple method of altering the microstructure of inkjet-printed films is by altering the rheological properties of the precursor ink. A change in viscosity, effected by a change in solids loading, results in microstructures with more or less porosity/density depending on the amount and dispersion of solids. In this work, the cathode microstructure was tailored by altering the solids loading in the precursor cathode inks. This article summarizes the results of this study.

Experimental

Ink preparation.— The method of ink preparation for the anode interlayer, NiO-YSZ (NiO, NexTech and YSZ, 8 mol %, Tosoh TZ-8YS), and electrolyte (8 mol %, Tosoh TZ-8YS) was presented in Ref. 15 and 16. The same method was adopted for the cathode interlayer strontium-doped lanthanum manganate (LSM, $La_{0.8}Sr_{0.2}MnO_3$, Nextech)–YSZ and the cathode current collection layer, LSM. α-Terpineol was used as the solvent for the ink slurries. Polyvinyl butyral (PVB), butyl benzyl phthalate (BBP), and polyalkalyne glycol (PAG) were utilized as binder and plasticizer constituents. The composition of the inks for the current study is shown in Table I. Viscosity measurements for the various ink formulations were obtained using a Rheolab QC (Anton-Paar) rheometer.

Printing.— Printing of the layers was carried out using a Dimatix DMP 2831 inkjet printer. A jetting profile comprising a 32 V, 2.944 μs firing pulse with a frequency of 3 kHz was used for printing all layers, including the anode functional layer, the electrolyte, the cathode functional layer, and the cathode current collection layer. Each layer was typically produced through multiple passes in succession, with the inkjet head operating at a temperature above ambient. The choice of the inkjet head/cartridge temperature was dictated by the different drying rates of the printed layers for composite vs single component precursors. A green tape cast material with a composition of 55 wt % NiO/45 wt % YSZ (ESL Electroscience, King of Prussia, PA) bisque fired at 950°C was used as the anode support/substrate for all printing.

Anode interlayer.— A total of 10 passes of the anode interlayer were printed over the anode support using the anode interlayer ink. The internal cartridge temperature was set to 58°C, and the platen/substrate temperature was maintained at room temperature, and after every two passes was raised to 100°C to allow intermediate drying. Finally, the platen temperature was raised to 120°C for complete drying.

Electrolyte.— Three sets of electrolytes were printed. For the first set of electrolytes (for use in electrochemical cell testing), an ink composition containing 2.4 g (4 vol % solids) of YSZ was used. Eight passes of electrolyte were printed over the dried anode interlayer using an electrolyte ink in a manner similar to that used in the anode interlayer. The internal cartridge temperature was set to 48°C. A second set of electrolytes was printed using an ink composition containing 2.4 g (4 vol % solids) of YSZ in a manner identical to the first set, except for changing the platen/substrate temperature during printing from room temperature to 35°C for one batch and 75°C for another batch. A third set of electrolytes using YSZ ink composition containing 1.2 g (2 vol % solids) was also printed in an identical manner to the first set. All drying procedures and cartridge temperature for the second and third sets were kept identical to the first set. The three sets of electrolytes were used to study the impact of platen/substrate temperature and solids loading on the microstructure of the printed film. Once the electrolyte deposition was complete, the anode/anode interlayer/electrolyte structure was cofired at 1400°C for 2 h.

[z] E-mail: mary.ayyadurai.ctr@wpafb.af.mil

Table I. Ink compositions.

Constituent	Anode interlayer (g)	Electrolyte (g)	Cathode interlayer (g)	Cathode current collector layer (g)
α-Terpineol	10	10	10	10
YSZ	0.3	2.4,1.2	1.2	0
NiO	0.3	0	0	0
LSM	0	0	1.2	1.2
PAG	0.01	0.01	0.01	0.01
BBP	0.01	0.01	0.01	0.01
PVB	0.01	0.01	0.01	0.01

Cathode layers.— Printed cathode interlayer films were prepared with 10 successive passes of the cathode interlayer ink on a circular area over the cofired electrolyte of the first set. The internal cartridge temperature for printing was 58°C. The platen temperature was maintained at 100°C while printing. Finally, the platen temperature was raised to 120°C for complete drying. After the drying of the cathode interlayer, a cathode current collector layer was prepared by 20 successive passes of the pure LSM ink over the cathode interlayer in a manner similar to that used for the cathode interlayer. The internal cartridge temperature for printing was 48°C. The printed cell was again sintered at 1200°C for 1 h. The diameters of the cathode functional layer/cathode were 13 mm with the cathode area considered as the active area for the cell and used as the basis for the calculation of current density. These cells are designated as PR here.

For comparison with a printed cathode performance, a cell with partly pasted (cathode interlayer and cathode current collection layer) and partly printed (anode interlayer and electrolyte) components was made. This cell is designated as PRS here. The printing of its anode interlayer and electrolyte was identical to that of PR. The cathode interlayer consisting of 50/50 wt % of LSM/YSZ was prepared by ballmilling the LSM and YSZ powders, solvents, plasticizer, and dispersant into a highly viscous ink for several hours and then hand painting over the printed electrolyte. The coupon was then sintered at 1200°C for 1 h. Finally, a cathode current collection layer was hand-painted using a pure LSM in an ink (LSM paste, NexTech) and sintered at 1200°C.

Cell testing and microstructure.— Details of the cell assembly and electrochemical impedance measurements are given in Ref. 15 and 16. Electrochemical testing (dc polarization and ac impedance measurements) was done with dry hydrogen as the fuel and air as the oxidant in the temperature range from 650 to 850°C. After testing, the cells were cooled to room temperature with the anode side exposed to a reducing atmosphere of forming gas. Post-testing morphology and microstructural study was carried out using a Quanta FE 600 field-emission scanning electron microscope (SEM).

Results and Discussion

Ink viscosity and shelf life.— Table I shows the ink compositions used in the current study. To sustain stable ink formulations, solids loading was kept low (<5 vol %), resulting in low viscosity formulations. In single component inks (YSZ and LSM), the ink retained a visually stable suspension for a period of 2–3 weeks. The cartridges containing these inks were observed to produce stable jets for longer than 2–3 weeks, suggesting reasonably stable suspension properties as excess flocculation or sedimentation in the ink is likely to result in clogging of the print head. In composite inks (anode interlayer and cathode interlayer), the shelf life of the anode interlayer was about 3–4 weeks, while the cathode interlayer ink required periodic homogenization.

Detailed behavior of viscosity of the inks used in the current study is discussed in Ref. 16. The major change in the current study, with respect to inks, is that of the cathode interlayer ink. The LSM/YSZ loading in the current study has been increased to 2.4 g (4 vol %) from 0.3 g (0.5 vol %) in the previous study. Increased solids loading resulted in higher viscosities. The cathode interlayer ink viscosity changes from 6 mPa s at printing temperature (internal cartridge temperature) for 0.3 g (0.5 vol %) to 8 mPa s for 2.4 g (4 vol %). The electrolyte ink with a composition of 2.4 g (4 vol % solids) had a viscosity of 7.8 mPa s, and the composition containing 1.2 g (2 vol % solids) of YSZ had a viscosity of 7.2 mPa s at printing temperature. The room-temperature viscosity of the inks used ranged from 58 to 73 mPa s. The overall trends in viscosity with shear rate for all the ink used in the current study are similar to that observed in the previous study.[16]

Cell performance and microstructure.— Figure 1a and b shows the scanning electron micrograph of the cross section of the typical PR and PRS, respectively. A dense electrolyte (about 16 μm in thickness) and porous cathode interlayers and cathode current collection layers can be seen. The anode interlayer is indistinguishable from the anode support (even at higher magnifications not shown here). Perhaps this is because the composition of the support (55/45 wt % NiO/YSZ) and the anode interlayer (50/50 wt % NiO/YSZ) is similar, and hence the transition in porosity between these components is minimal. The printed cathode appears thicker than the pasted cathode. Figure 2a-c shows the current and power density characteristics of the three identically printed PR cells and Fig. 2d shows the current and power density characteristics of a typical PRS cell at temperatures ranging from 650 to 850°C. For all cells, the open-circuit voltage (OCV) is observed to vary from 1.10 to 1.14 V depending on the temperature. As the temperature increases from 650 to 850°C, the current and power densities increase. The maximum power density at 850°C is 0.46 W/cm^2 for cells a and b. For cell c, the maximum power density is 0.43 W/cm^2. For the printed cathode cells, it was observed that when the cathode thicknesses (cathode interlayer and cathode current collection layers) were very close for the different cells, the performance was identical. Typically the printed cathode thickness (cathode interlayer and cathode current collection layers together) was between 40 and 60 μm. The performance for cell c in the temperature range from 650 to 750°C is lower compared to that of cells a and b, while the performance at 800 and 850°C was comparable with that of cells a and b. This

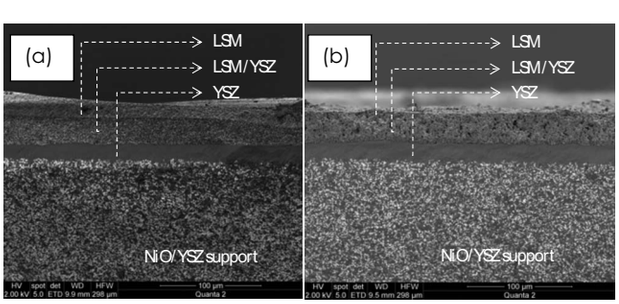

Figure 1. SEM cross-sectional view of typical (a) PR cell (all nonsupported layers inkjet printed) and (b) PRS cell (identical to PR cell but with hand-pasted cathode). LSM cathode current collection layer, LSM/YSZ cathode interlayer, and YSZ electrolyte layer.

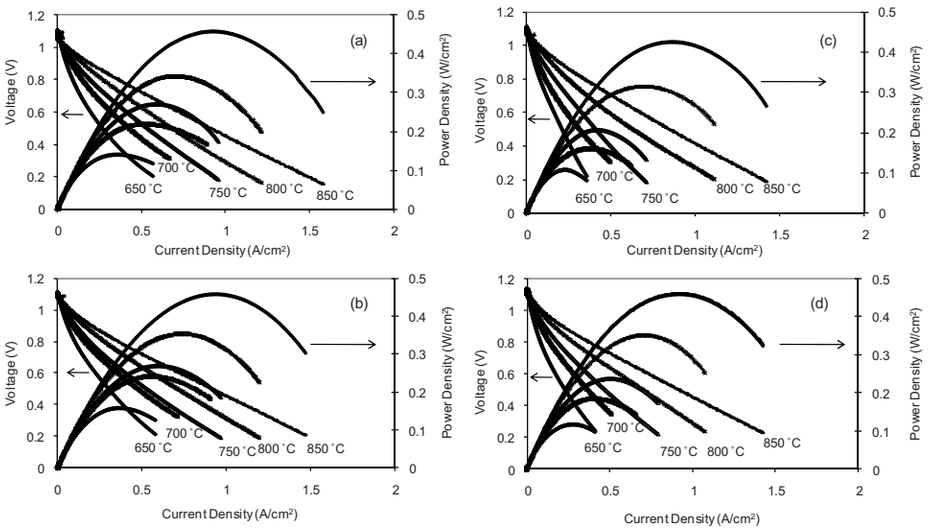

Figure 2. Performance curves of [(a)–(c)] three identical PR cells and (d) a typical PRS cell.

behavior was observed when the printed cathode thickness was in the range of 60–75 μm. These differences in low temperature behavior may be attributed to small differences in the cathode thickness as the LSM-based cathode's performance usually improves with increasing temperatures around 800°C. A highly reproducible cathode interlayer thickness required an accurate control of the substrate temperature and drying methods/solvent evaporation rate. The maximum power density at 850°C is 0.45 W/cm^2 for cell d. The total thickness of the typically pasted cathode (cathode interlayer and cathode current collection layers) was 30–40 μm. Thus, Fig. 2 shows that the performance of the PR cells is comparable to that of a typical PRS cell. Figure 3a and b shows the impedance plot at open circuit for typical PR and PRS cells, respectively. The decrease in overall impedance of the cells with increasing temperature is due to the increased ionic conductivity of the electrolyte and the decreased electrode activation overpotential. The trends in impedance point to a slightly larger polarization resistance (R_p is the difference in intercept between low and high frequencies) for the PRS cell compared to PR at all temperatures from 650 to 850°C. The small difference in impedance between the two cells may be attributed to differences in cathode microstructure. Closer examination of the cathode layers in PR and PRS cells in Fig. 4 suggests differences in both layer thicknesses and qualitative differences in microstructure. Strict comparisons of the printed and pasted cathode microstructures require further optimization of the printed cathode interlayer and cathode current collection layers thicknesses and quantitative assessment of microstructures.

Impact of ink rheology and inkjet printing parameters on porosity/density of layers.— In the inkjet deposition process, the ejected droplet velocity, size and stability, as well as the shape of the droplets impinging on the substrate, depend on the rheological properties such as viscosity and surface tension.[18] For a given driving waveform (characterized by the amplitude, frequency, and firing pulse width), the velocity and mass of the droplet increase with decreasing viscosity.[19] Thus, a combination of jetting parameters and fluid properties determines the drop formation. The characteristic of the drop, combined with the substrate characteristics (substrate roughness and temperature), determines the green density/porosity/quality of the printed films. High temperature firing determines the final density/porosity of the SOFC components. Figure 5 shows the impact of platen temperature (a factor that determines solvent evaporation rate) during the printing process on the sintered microstructure. Micrograph (a) shows the surface of the electrolyte

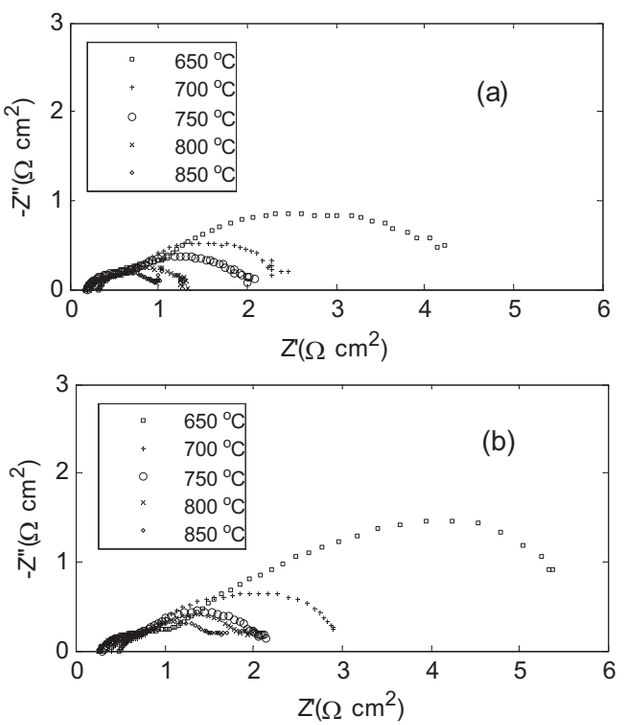

Figure 3. Impedance plot (at OCV) of (a) a typical PR cell and (b) a typical PRS cell (frequency increases from right to left).

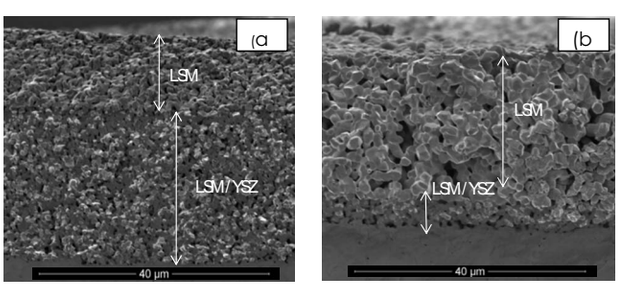

Figure 4. SEM cross-sectional view of cathodes of typical (a) PR and (b) PRS cells.

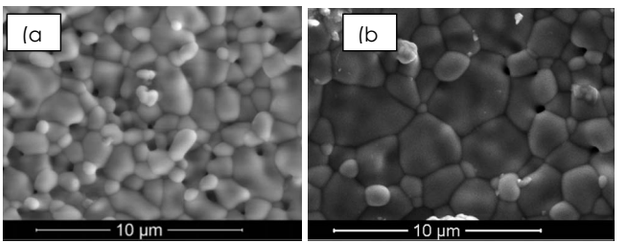

Figure 5. SEM view of the surface of the electrolyte (sintered at 1400°C) printed (from ink with a solid loading of 2.4 g YSZ) with substrate/platen at (a) 35 and (b) 75°C during printing.

(sintered at 1400°C) printed using ink with a solid loading of 2.4 g of YSZ (4 vol % solids) and substrate/platen held at 35°C. Micrograph (b) shows the surface of the electrolyte (sintered at 1400°C) printed using ink with solids loading of 2.4 g of YSZ (4 vol % solids) and substrate/platen held at 75°C. The grain size has increased and the number of pores at the grain boundaries has decreased, suggesting an overall increase in the density of the film. Figure 6 shows the impact of solids loading (viscosity) in the electrolyte ink on the sintered microstructure. When the solids loading of YSZ in the electrolyte ink is changed from 2.4 g (4 vol % solids and 7.8 mPa s viscosity at the cartridge temperature) to 1.2 g (2 vol % solids and 7.2 mPa s at the cartridge temperature), the grain size increases and fewer pores are seen, suggesting better sinterability and hence higher density in the cofired electrolyte. Figures 5 and 6 highlight the impact of both the rheological property (such as viscosity) and printing process parameter such as solvent evaporation rate on the microstructure of the films. A similar study for cathode components is underway. The impact of these parametric changes on the microstructure and electrochemical performance is the subject of a future publication.

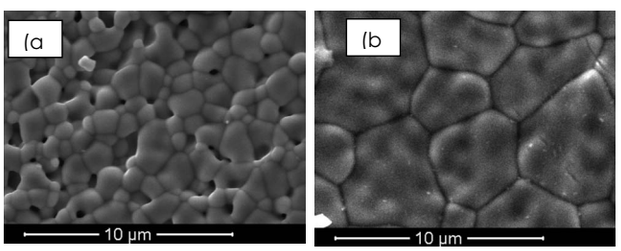

Figure 6. SEM view of the surface of the electrolyte (sintered at 1400°C) printed with substrate/platen at room temperature using YSZ ink composition with solid loadings of (a) 2.4 g (4 vol % solids) and (b) 1.2 g (2 vol % solids).

Conclusion

Inkjet printing can be used to produce complete SOFCs with an electrochemical performance consistent with traditional processing methodologies. Printed cells tested in hydrogen produced a stable voltage of 1.1 V and exhibited a maximum power density ranging from 0.43 to 0.46 W/cm^2 at 850°C. This performance matched the performance of a cell identical to printed cells but with hand-pasted cathode layers. Altering the rheological property of the ink and/or printing process parameter alters the microstructure of printed layers. With the ability to produce functional cells demonstrated, inkjet processing techniques can be explored to provide greater flexibility in the design of tailored cell structures, possibly enabling the development of patterned multilayer cells or advanced cell/stack configurations. Furthermore, the cost effectiveness of this process could provide a pathway toward a more rapid commercialization of SOFC technology.

Acknowledgments

The authors acknowledge the help of Thomas Jenkins with the materials processing and cell fabrication and Frederick Meisenkothen for his assistance with the microscopy work.

References

1. N. Q. Minh, *J. Am. Ceram. Soc.*, **76**, 563 (1993).
2. S. Singhal, *Solid State Ionics*, **135**, 305 (2000).
3. B. C. H. Steele, *Solid State Ionics*, **134**, 3 (2000).
4. T. Kenjo and M. Nishiya, *Solid State Ionics*, **57**, 295 (1992).
5. T. Kenjo, S. Osawa, and K. Fujikawa, *J. Electrochem. Soc.*, **138**, 349 (1991).
6. C. Holtappels and C. Bagger, *J. Eur. Ceram. Soc.*, **22**, 41 (2002).
7. P. Holtappels, C. Sorof, M. C. Verbraeken, S. Rambert, and U. Vogt, *Fuel Cells*, **6**, 113 (2006).
8. M. Wetzko, A. Belzner, F. J. Rohr, and F. Harbach, *J. Power Sources*, **83**, 148 (1999).
9. T. S. Lai and S. A. Barnett, *J. Power Sources*, **147**, 85 (2005).
10. M. R. Pillai, D. Gostovic, I. Kim, and S. Barnett, *J. Power Sources*, **163**, 960 (2007).
11. J. Will, A. Mitterdorfer, C. Kleinlogel, D. Perednis, and L. J. Gauckler, *Solid State Ionics*, **131**, 79 (2000).
12. L. R. Pederson, P. Singh, and X.-D. Zhou, *Vacuum*, **80**, 1066 (2006).
13. V. G. Shah, D. J. Hayes, and D. B. Wallace, in *Fuel Cell Electronics Packaging*, K. Kuang and K. Easler, Editors, Chap. 11, Springer, New York (2007).
14. A. D. Taylor, E. Y. Kim, V. P. Humes, J. Kizuka, and L. T. Thompson, *J. Power Sources*, **171**, 101 (2007).
15. D. Young, A. M. Sukeshini, R. Cummins, H. Xiao, M. Rottmayer, and T. Reitz, *J. Power Sources*, **184**, 191 (2008).
16. A. M. Sukeshini, R. Cummins, T. Reitz, and R. Miller, *J. Am. Ceram. Soc.*, In press. [DOI: 10.1111/j.1551-2916.2009.03349.x]
17. A. M. El-Toni, T. Yamaguchi, S. Shimizu, Y. Fujishiro, and M. Awano, *J. Am. Ceram. Soc.*, **91**, 346 (2008).
18. H. P. Lee, *J. Imaging Sci. Technol.*, **42**, 49 (1998).
19. Dimatix DMP 2831 ink-jet printer user manual.